The Plant Cell, Vol. 27: 3099–3111, November 2015, www.plantcell.org

Arabidopsis LEAFY COTYLEDON1 Mediates Postembryonic Development via Interacting with PHYTOCHROME-INTERACTING FACTOR4[OPEN]

Mingkun Huang,[a,b] Yilong Hu,[a,b] Xu Liu,[a] Yuge Li,[a] and Xingliang Hou[a,1]

[a] Key Laboratory of South China Agricultural Plant Molecular Analysis and Genetic Improvement, South China Botanical Garden, Chinese Academy of Sciences, Guangzhou 510650, China
[b] University of the Chinese Academy of Sciences, Beijing 100049, China

ORCID IDs: 0000-0003-1970-0608 (X.L.); 0000-0002-3964-2372 (X.H.)

Plants undergo postembryonic growth during the developmental transition from germinating seeds to seedlings. Recent studies suggest LEAFY COTYLEDON1 (LEC1), initially identified as a central regulator in embryogenesis and seed maturation in *Arabidopsis thaliana*, plays a distinct role in postembryonic development. However, the mechanism by which LEC1 regulates nonembryonic development still remains elusive. In this study, we observed etiolation-related phenotypes in early seedlings of *lec1* mutants and inducible *LEC1* overexpression transgenic lines. Consistent with this, LEC1 promotes the expression of hypocotyl elongation-related genes in a darkness-dependent manner in spite of the comparable *LEC1* transcript levels in the light- and dark-grown seedlings. Furthermore, we show that LEC1 interacts with PHYTOCHROME-INTERACTING FACTOR4 (PIF4), a major transcription modulator in postgermination development, to interdependently regulate hypocotyl elongation-related genes via direct binding to G-box element in the dark. Moreover, loss of *LEC1* function suppresses the elongated hypocotyl phenotype of *PIF*-overaccumulating plants; conversely, inducible overexpression of *LEC1* does not rescue the short hypocotyl in *pif4* mutants. Our findings reveal that LEC1 acts as a coactivator of PIFs in transcriptional regulation during postembryonic growth, providing a possible mechanism by which plants fine-tune morphological development for their survival during the transition from the embryonic phase to seedling establishment.

INTRODUCTION

Plants have evolved sophisticated sensory systems to perceive changes in light quality, intensity, direction, and periodicity (Chen et al., 2004). Seedlings grown in the light develop short hypocotyls and open cotyledons, which is referred to as photomorphogenesis. However, during the developmental transition from germinating seeds to seedlings, plants kept in darkness adopt a skotomorphogenic or etiolation program, including rapid elongation of the hypocotyl, tightly folded apical hook, and closed cotyledons, ensuring that limited seed reserves are used effectively to survive until the plant is exposed to light (Von Arnim and Deng, 1996; Josse and Halliday, 2008).

PHYTOCHROME INTERACTING FACTORs (PIFs), a subgroup of basic helix-loop-helix (bHLH) transcription factors, act as central modulators in the postgermination stage (Castillon et al., 2007; Bae and Choi, 2008; Leivar and Quail, 2011; Leivar and Monte, 2014). Mutants deficient in PIFs, such as *pif3*, *pif4*, and the *pif1 pif3 pif4 pif5* (*pifq*) quadruple mutant, show partial or constitutive photomorphogenesis in the dark; overexpression of *PIF3*, *PIF4*, or *PIF5* leads to high induction of genes involved in skotomorphogenesis and relevant etiolation phenotype, suggesting PIFs contribute to the maintenance of skotomorphogenesis state (Huq and Quail, 2002; Kim et al., 2003; Leivar et al., 2008). Previous studies demonstrated that PIFs are destabilized in light-grown seedlings, which is the result of the light-triggered nuclear relocalization of phytochromes (Khanna et al., 2004; Al-Sady et al., 2006). For example, phytochrome B (phyB) is a red/far-red photoreceptor involved in the regulation of deetiolation and its null mutant shows an etiolation-like phenotype. Red light induces the Pr form of phyB into the active Pfr form, which relocates to the nucleus and interacts with PIFs through the conserved active phytochrome binding motif. The interaction between phyB and PIFs results in phosphorylation of PIFs and their subsequent degradation by the 26S proteasome, thus relieving the repression of light responses (Leivar et al., 2008; Leivar and Quail, 2011; Leivar and Monte, 2014). Conversely, light-induced phosphorylation of PIFs is also necessary for the degradation of phyB. A recent study reported that recruitment of LRB E3 ubiquitin ligases to the PIF3-phyB complex facilitates concurrent polyubiquitination and degradation of PIF3 and phyB, which assures destruction of the receptor and its immediate signaling partner when "lighting up" in plants (Ni et al., 2014).

Besides the well-characterized phyB-PIF regulatory module in the light, several PIF cofactors, such as DELLA, BZR1, HDA15, and PKL, affect PIFs' transcriptional activity on targets via epigenetic regulation and thus allow the integration of light and other cellular pathways (de Lucas et al., 2008; Feng et al., 2008; Oh et al., 2012; Zhang et al., 2014). Especially, in addition to functioning in hypocotyl elongation in light conditions, the chromatin-remodeling factor PKL also negatively regulates expression of *LEAFY COTYLEDON1*

[1] Address correspondence to houxl@scib.ac.cn.
The author responsible for distribution of materials integral to the findings presented in this article in accordance with the policy described in the Instructions for Authors (www.plantcell.org) is: Xingliang Hou (houxl@scib.ac.cn).
[OPEN]Articles can be viewed online without a subscription.
www.plantcell.org/cgi/doi/10.1105/tpc.15.00750

(*LEC1*) and the embryonic program, implying a possible mechanistic connection between embryogenesis and light signaling (Zhang et al., 2012; Jing et al., 2013).

LEC1, one of the first nuclear factor Y (NF-Y) family members identified in plants, acts as a central regulator controlling embryogenesis and seed maturation in *Arabidopsis thaliana* (Meinke et al., 1994; West et al., 1994; Parcy et al., 1997; Lotan et al., 1998; Harada, 2001). Consistent with this, *LEC1* is predominantly expressed during early and late stages of seed development (Le et al., 2010). Strong evidence supporting the pivotal role of LEC1 in embryo development came with the finding that ectopic *LEC1* expression was sufficient to induce somatic embryogenesis from vegetative cells (Lotan et al., 1998). In contrast, the *LEC1* null mutant causes a pleiotropic phenotype, including abnormal embryo and seed desiccation intolerance, defects in reserve accumulation, leafy cotyledons, and a reduced capability for hypocotyl elongation, indicating that in addition to its vital function in embryogenesis, LEC1 also plays a distinct role in postembryonic development (Lotan et al., 1998; Harada, 2001; Brocard-Gifford et al., 2003). However, the molecular mechanism of such nonembryonic functions of LEC1 still remains elusive.

In this study, we isolated a *LEC1* knockdown mutant that mostly phenocopies the *LEC1* null allele but with higher desiccation tolerance in mature seeds, which provides a more efficient genetic tool to examine LEC1 function in plants. Primarily, we found that LEC1 and PIF4, one of the major transcription modulators in skotomorphogenesis, interdependently regulate hypocotyl elongation of early seedlings in a darkness-dependent manner. LEC1 binds to the G-box in the promoters of hypocotyl-related genes via protein-protein interaction with PIF4 in Arabidopsis. Our findings reveal that LEC1 acts as a coactivator of PIFs in transcriptional regulation of postembryonic growth, providing a possible mechanism by which plants can fine-tune morphological development for their survival during the transition from the embryonic phase to seedling establishment.

RESULTS

Identification and Characterization of the *lec1-4* Mutant

To investigate the *LEC1*-mediated regulatory mechanisms acting during the transition from seed to seedling establishment, we identified a mutant (SALK_095699) in the Columbia (Col) background containing a T-DNA insertion in the *LEC1* intron from the ABRC (Figures 1A and 1B). We named this mutant *lec1-4*, based on our subsequent characterization described below. RT-PCR showed that the expression of *LEC1* only remained low in abundance in developing *lec1-4* mutant seeds in comparison to highly expressed *LEC1* in the wild type (Figure 1C). Similar to previously reported *LEC1* null mutants such as *lec1-3*, the typical pleiotropic phenotypes of *lec1-4*, including defective embryos, abnormal seeds, developed trichomes on cotyledons, short hypocotyls, and less apical hook formation in the dark (Figures 1D to 1G; Supplemental Figures 1A and 1B). However, some of the *lec1-4* phenotypes are weaker than those in *lec1-3* null mutants, probably due to the leaky expression of *LEC1* (Figure 1C). For example, ~90% freshly harvested mature seeds from the *lec1-4* mutants are viable in spite of reduced germination rate following longer storage, whereas the seed embryo of the *lec1-3* null allele is desiccation-intolerant and has to be rescued before maturation in order to continue growth (Figures 1H and 1I; West et al., 1994). Thus, it is more convenient for us to get *lec1-4* homozygous recessive plants whenever needed. In addition, in *lec1-4* mutants, the amount of trichomes developed on the cotyledons was greatly variable and a few of seedlings resembling the wild type can also be observed (Supplemental Figure 1C). These results indicate that the defective phenotype observed is due to knockdown of *LEC1*. This is further corroborated by a complementation test in which a 3.8-kb genomic fragment of *LEC1* fused with a 3×FLAG tag (*pLEC1:LEC1-FLAG*) was able to rescue the *lec1* typical phenotypes (Supplemental Figures 2A to 2F). Taking these observations together, we defined this mutant as a *lec1* allele and designated it *lec1-4*. Because of the high viability of seeds after desiccation, *lec1-4* mutant is more suitable to be used for genetic analysis.

LEC1 Functions in Postembryonic Development

LEC1 acts as a crucial regulator of embryogenesis and seed development (Meinke et al., 1994; West et al., 1994; Parcy et al., 1997; Lotan et al., 1998; Harada, 2001). However, observation of the short hypocotyl and reduced apical hook formation in *lec1* mutants suggests a definite role of LEC1 in etiolated growth during postembryonic development (Figures 1F and 1G; Supplemental Figure 1B; Brocard-Gifford et al., 2003; Junker and Bäumlein, 2012). To further confirm whether LEC1 functions in etiolation, we first examined the expression of *LEC1* in 5-d-old seedlings grown under light and dark conditions. The results showed that *LEC1* had comparable expression in seedlings grown in the light and dark; it also had little expression in rosette leaves and high expression in developing seeds (Figure 2A). Immunoblot assay of *lec1-4 pLEC1:LEC1-FLAG* transgenic seedlings demonstrated that LEC1 protein expression was consistent with its transcription pattern, and light had no effect on LEC1 abundance (Figure 2B). Next, we generated transgenic plants harboring *GUS* driven by an ~2-kb fragment of the *LEC1* promoter region (*pLEC1:GUS*) to examine the tissue-specific expression of *LEC1*. Consistent with the expression pattern of *LEC1*, GUS staining was found in seedlings grown in the light and dark and developing seeds but barely in rosette leaves (Figure 1C). These results imply the potential role of LEC1 in early seedling development.

To learn whether LEC1 regulates the expression of genes involved in etiolated growth, we measured transcript levels of *IAA19*, *YUC8*, *ATHB-2*, and *IAA29*, four typical genes involved in dark-induced hypocotyl elongation (Kunihiro et al., 2011; Sun et al., 2012; Zhang et al., 2013), in Col and *lec1-4*. At 6 h after the transition from light to darkness, expression of all four genes was dramatically induced in wild-type seedlings. In contrast, increase in transcript levels of these genes in darkness was significantly compromised in *lec1-4* mutants, indicating that LEC1 is important for activation of hypocotyl elongation-related genes in the dark (Figure 2D).

Since constitutive expression of *LEC1* could cause serious defects including embryo lethality or embryo-like structures in vegetative tissues (Lotan et al., 1998; Mu et al., 2008; Junker and Bäumlein, 2012), we employed an estradiol-inducible transgenic

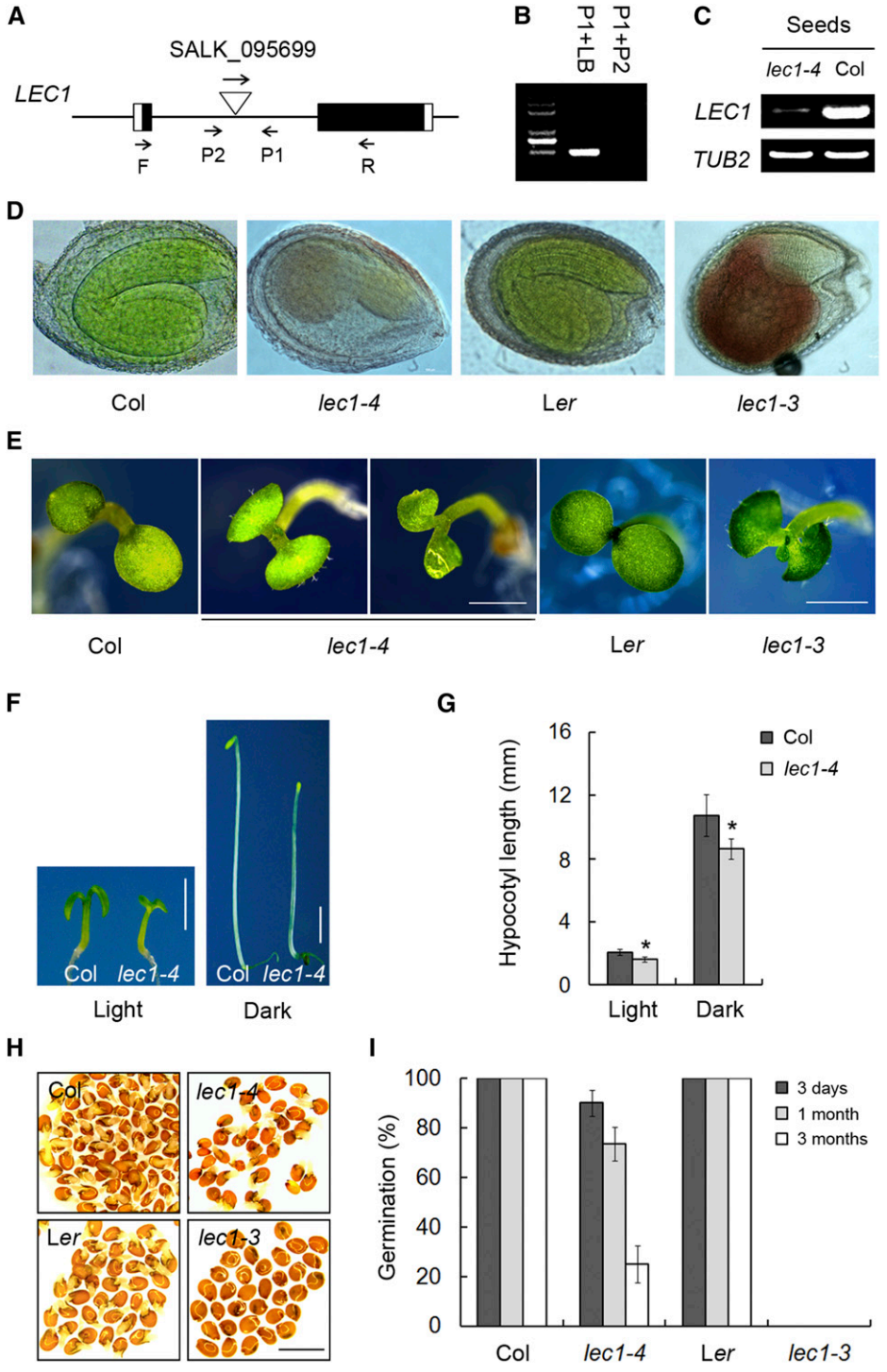

Figure 1. Identification of a *LEC1* Knockdown Allele in Arabidopsis.

(A) Schematic diagram showing the T-DNA insertion site in *lec1-4* (SALK_095699). Exons are represented by boxes and introns by lines between the boxes. Black boxes represent the *LEC1* coding regions.

(B) PCR of genomic DNA confirms that *lec1-4* is a homozygous insertion mutant. The primers used are shown in **(A)**. LB indicates the T-DNA left border primer.

(C) *LEC1* expression is low in *lec1-4* in comparison to the wild type by RT-PCR using the primers F and R shown in **(A)**. Total RNA was isolated from developing seeds (6 d after pollination) of *lec1-4* and Col plants.

plant harboring *pER10:LEC1-MYC* to further verify *LEC1* function. RT-PCR and immunoblot analyses showed that *LEC1* expression was promptly induced and specific LEC1 protein accumulation was detected in estradiol-treated *pER10:LEC1-MYC* plants (Supplemental Figures 3A and 3B). As expected, estradiol induced longer hypocotyls in *pER10:LEC1-MYC* seedlings, while hypocotyl elongation was not affected in estradiol-treated wild type and mock-treated *pER10:LEC1-MYC* (Figures 2E and 2F). To further confirm the regulation of LEC1 on hypocotyl elongation-related genes, we measured transcript levels of *IAA19*, *YUC8*, *ATHB-2*, and *IAA29* in 3-d-old *pER10:LEC1-MYC* seedlings that were transferred to the darkness or continuous light over a time course with estradiol treatment. Consistent with the phenotype of the transgenic plant, *IAA19*, *YUC8*, *ATHB-2*, and *IAA29* transcript levels were dramatically elevated by induction of LEC1 in the dark (Figure 2G). Interestingly, under light conditions, we detected no significant promotion of expression of these genes (Supplemental Figure 3C), suggesting that LEC1 regulates hypocotyl elongation in a dark-dependent manner.

LEC1 Interacts with PIF4

NF-Y subunits interact with other transcription factors to modulate gene expression in plant development and stress responses (Liu and Howell, 2010; Hou et al., 2014). LEC1 belongs to the NF-YB family; thus, we reasoned that LEC1 might function with other partners in the regulation of hypocotyl elongation during postembryonic development. PIF transcription factors, including PIF1, PIF3, PIF4, and PIF5, function as central modulators in skotomorphogenic growth, and *pif* loss-of-function mutants show reduced hypocotyl length, like *lec1-4* mutants (Supplemental Figures 4A and 4B). Also, PIFs directly regulate expression of *IAA19*, *YUC8*, *ATHB-2*, and *IAA29* (Supplemental Figure 4C; Kunihiro et al., 2011; Hornitschek et al., 2012; Oh et al., 2012; Sun et al., 2012; Zhang et al., 2013); thus, it is possible that LEC1 may coregulate hypocotyl elongation with PIFs. Since overexpression of *LEC1* did not affect *PIF4* transcript levels (Supplemental Figure 4D), we tested the protein interaction between LEC1 and PIFs using a yeast two-hybrid assay. Strikingly, the results demonstrated a strong interaction between LEC1 and PIF4 and a weaker interaction between LEC and PIF3, but detected no interaction between LEC1 and PIF1 or PIF5 or between L1L, the closest homolog of LEC1 in Arabidopsis, and all indicated PIFs (Supplemental Figure 5). In our observations, the *L1L* null mutant (*l1l-1*) showed less of a change in hypocotyl length, suggesting that *L1L* is not involved in postembryonic growth (Supplemental Figure 6). We further generated two truncated versions of LEC1 and three versions of PIF4 to identify the functional domains required for the interaction (Figure 3A). The B-domain in LEC1 is a conserved domain in the NF-YB family and probably functions in NF-Y trimerization (Calvenzani et al., 2012; Hackenberg et al., 2012). The bHLH domain in PIFs was reported to be a DNA binding domain (Toledo-Ortiz et al., 2003). We found that neither the B-domain of LEC1 nor the bHLH domain of PIF4 was involved in the protein interaction; rather, the C-terminal domains of LEC1 and PIF4 were sufficient and necessary for their interaction (Figure 3B). This indicates that the LEC1-PIF4 interaction may not influence PIF4-DNA binding and may not compete for NF-YA/LEC1/NF-YC trimerization. We next performed pull-down assays to verify the interaction between PIF4 and LEC1, using purified GST- and His-tagged proteins. Again, we found that GST-PIF4, but not GST alone, precipitated His-LEC1 in vitro (Figure 3C). In addition, bimolecular fluorescence complementation (BiFC) analysis revealed the interaction of LEC1 and PIF4 in the nuclei of living plant cells (Figure 3D). Coimmunoprecipitation of protein extracts from *pLEC1:LEC1-FLAG 35S:PIF4-HA* seedlings further confirmed the interaction between LEC1 and PIF4 in vivo (Figure 3E). Taken together, these results indicate that LEC1 might regulate plant postembryonic growth through its interaction with PIF4.

LEC1 and PIF4 Coregulate Hypocotyl Elongation-Related Genes via Direct Binding to the G-Box

Previous studies showed that PIFs promote skotomorphogenesis in the dark via specific binding to G-box or E-box variants in downstream genes (Huq and Quail, 2002; Hornitschek et al., 2012; Oh et al., 2012; Zhang et al., 2013). To learn how the interaction between LEC1 and PIF4 regulates the expression of genes involved in hypocotyl elongation, we performed chromatin immunoprecipitation (ChIP) assays to measure the DNA enrichment of G-box in *IAA19* and *YUC8*, downstream genes of both LEC1 and PIF4 (Figure 2G; Supplemental Figure 4C). Consistent with previous reports, the results showed that PIF4 strongly bound to the G-box-containing regions at P1 and P3 in *IAA19* promoter and P2 in *YUC8* promoter (Figure 4B). Furthermore, a similar DNA enrichment pattern in *IAA19* or *YUC8* by the inducible LEC1-MYC protein was also detected in the dark-treated *pER10:LEC1-MYC* seedlings, whereas no significant binding of LEC1 to these genes was observed in light-grown plants (Figure 4C; Supplemental Figure 3D). ChIP analysis for *IAA29* and *ATHB-2*, two other downstream genes of LEC1 and PIF4 (Figure 2G; Supplemental Figure 4C), also showed similar results to those observed for

Figure 1. (continued).

(D) The *lec1* mutants exhibit abnormal embryos in comparison to the wild type. Bar = 1 mm.

(E) The *lec1* mutants develop trichomes on their cotyledons or have shrunken cotyledons in comparison to the wild type. Five-day-old seedlings grown in the light were used for investigation. Bar = 1 mm.

(F) Five-day-old seedlings of *lec1-4* mutants grown in the light or dark show shorter hypocotyls than the wild type. Bar = 2 mm.

(G) Hypocotyl length statistics of the wild type and *lec1-4* seedlings shown in **(F)**. Data represent mean ± SD of at least 30 seedlings. Asterisks indicate significant differences between Col and *lec1-4* mutants ($P < 0.05$, by Student's *t* test).

(H) Germination investigation of the freshly harvested dry seeds from Col, *lec1-4*, Landsberg *erecta* (L*er*), and *lec1-3*. Germination rate of seeds was measured after transfer to 22°C for 1 d from 4°C stratification.

(I) Germination rate of the Col, *lec1-4*, L*er*, and *lec1-3* seeds with a 3-d, 1-month, or 3-month storage period after harvest.

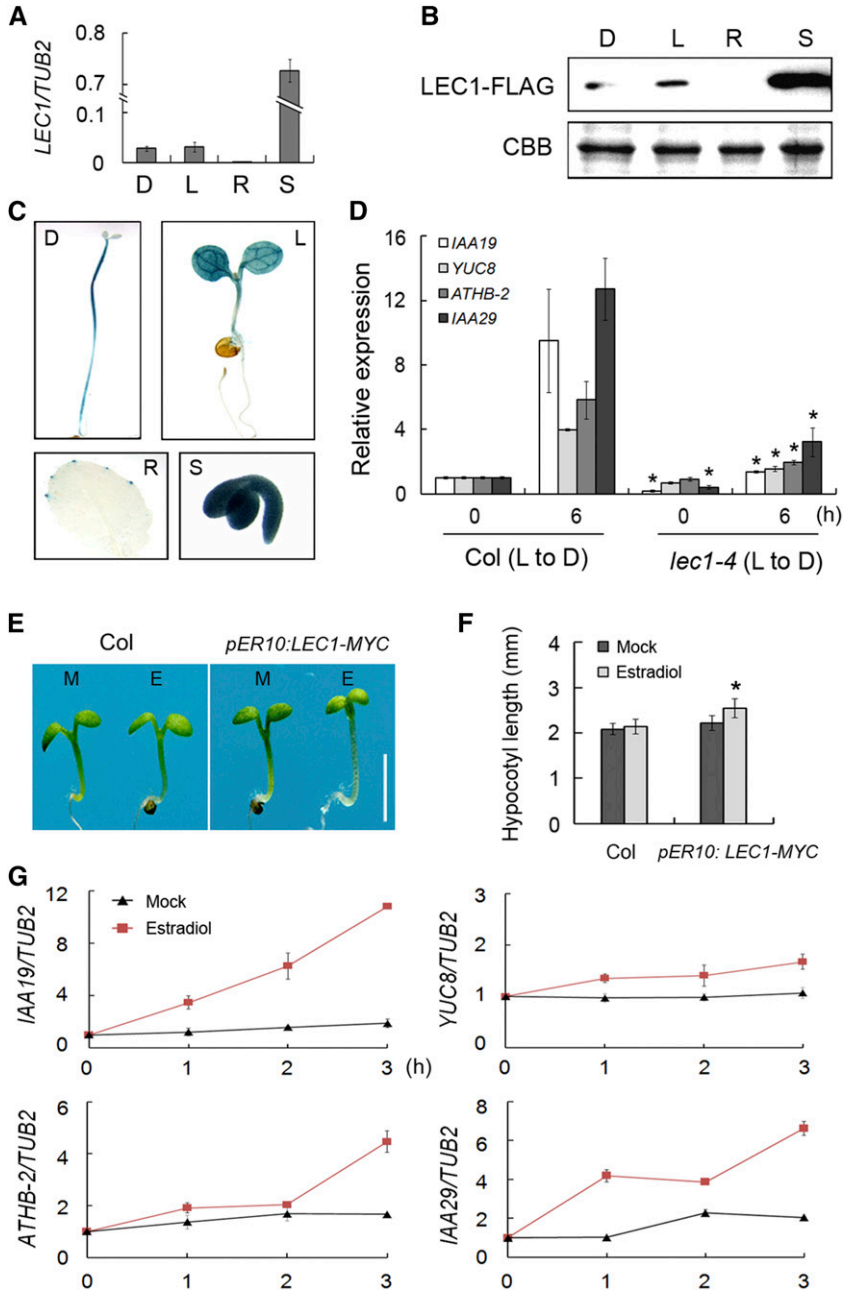

Figure 2. LEC1 Is Involved in Hypocotyl Elongation.

(A) Quantitative RT-PCR analysis showing *LEC1* expression in 5-d-old Col wild-type seedling grown in the dark (D) or in the light (L). Tissues from rosette leaves (R) and developing seeds (S) were used as negative and positive controls, respectively. The β-tubulin gene (*TUB2*) was amplified as an internal control.
(B) Immunoblot analysis of LEC1-FLAG protein expressed in tissues indicated in **(A)**. The *lec1-4 pLEC1:LEC1-FLAG* transgenic line was used to examine the LEC1 protein level. Coomassie blue staining (CBB) was used as a loading control.
(C) GUS staining of *pLEC1:GUS* transgenic plants. Tissues detected are indicated in **(A)**.
(D) Quantitative RT-PCR analysis showing repression of hypocotyl elongation-related gene expression in *lec1-4* in comparison to the wild type. Three-day-old *lec1-4* and Col seedlings grown in the light (0 h) or then transferred to darkness for 6 h (6 h) were harvested. Relative gene expression was calculated by comparing the values to that of Col at 0 h. *TUB2* was amplified as an internal control. Asterisks indicate significant differences between Col and *lec1-4* mutant ($P < 0.05$, by Student's *t* test). L to D, light to darkness.
(E) Hypocotyl length of the *pER10:LEC1-MYC* transgenic line. Five-day-old Col and *pER10:LEC1-MYC* seedlings grown in the light with 10 μM estradiol (E) or mock treatment (M) were used for investigation. Bar = 2 mm.

IAA19 and *YUC8* (Supplemental Figure 7), indicating that, in the dark, LEC1 and PIF4 cotarget the promoters of downstream genes probably via direct binding to G-box elements.

Since the LEC1 protein contains no identified DNA binding domain (Calvenzani et al., 2012), we speculated that LEC1 may bind to *IAA19* and *YUC8* by associating with PIF4, which contributes to the direct DNA affinity. To test this hypothesis, electrophoretic mobility shift assays (EMSAs) were performed using GST-PIF4 and His-LEC1 recombinant proteins and a biotinylated probe containing the G-box element in the P3 region of *IAA19*. The EMSAs also used a nonlabeled probe with mutated G-box as cold competitor (Supplemental Figure 8A). The results showed that PIF4 bound to the G-box element, whereas no binding occurred between LEC1 or GST protein and the P3 probe (Figure 4D). Remarkably, a band of slower mobility was detected when PIF4 was incubated with LEC1, indicating that these two proteins bind to the G-box as a heterodimer (Figure 4D).

To further examine the regulation of PIF4 and LEC1 on the expression of their target genes, we performed transient expression assays using ~2 kb of *IAA19* promoter fused to the GUS gene as a reporter (*pIAA19:GUS*). Effector constructs for PIF4-EYFP^N or LEC1-EYFP^C were expressed under the control of 35S promoter and transfected together with the reporter construct into Arabidopsis mesophyll protoplasts. Addition of either LEC1 or PIF4 significantly activated the expression of *IAA19*, whereas *IAA19* activation by LEC1 alone was abolished in *pifq* mutants (Figure 4E; Supplemental Figure 9), showing PIF4-dependent regulation of LEC1 on *IAA19*. Notably, higher GUS activity was detected when LEC1 and PIF4 proteins were coexpressed compared with that when either LEC1 or PIF4 was expressed alone (Figure 4E). However, when site-specific mutations were introduced into the two G-boxes (CACGTG to CACGgG) in *mpIAA19:GUS* (Supplemental Figure 8B), such disruption of G-box element dramatically reduced the expression of *IAA19* despite the presence of LEC1, PIF4, or both LEC1 and PIF4 (Figure 4E), indicating that the G-box element is essential for LEC1-PIF4-mediated activation of *IAA19*.

Taken together, these findings strongly support the idea that PIF4 and LEC1 coregulate downstream genes to regulate hypocotyl elongation.

LEC1 and PIF4 Act Interdependently in the Regulation of Hypocotyl Elongation

PIFs, including PIF1, PIF3, PIF4, and PIF5, function with overlapping redundancy in dark-grown seedlings to promote etiolated growth, and the photoactivated Phy-triggered degradation of PIFs induces deetiolation (Leivar et al., 2008). To further investigate the genetic role of LEC1 in postembryonic growth, we crossed *lec1-4* with *35S:PIF4*, *35S:PIF3-MYC*, and the *phyb* mutant in which the deetiolation response in the light is suppressed (Reed et al., 1993; Zhang et al., 2013). Hypocotyl elongation of *35S:PIF4*, *35S:PIF3-MYC*, and *phyb* was significantly reduced in the *lec1-4* background (Figures 5A and 5B; Supplemental Figures 10A and 10B). Consistent with this, expression of the hypocotyl elongation-related genes was also compromised in *lec1-4 35S:PIF4* plants, compared with that in *35S:PIF4* (Figure 5C). Together with the ChIP analysis, which showed that the association of PIF4-HA with G-box in *IAA19* and *YUC8* was attenuated in *lec1-4* mutants (Figure 5D), these results suggest that LEC1 promotes PIF-mediated hypocotyl elongation through enhancing DNA affinity of PIF4 to target genes.

In turn, we crossed *pER10:LEC1-MYC* to *pif4* to examine whether *LEC1* function in hypocotyl elongation depends on PIF4. Loss of *PIF4* function remarkably impaired the elongated hypocotyl induced by LEC1-MYC (Figures 5E and 5F), and expression of the hypocotyl elongation-related genes was consistently decreased in *pif4 pER10:LEC1-MYC* compared with that in *pER10:LEC1-MYC* when treated with estradiol in the dark (Figure 5G). Further ChIP assays showed that the DNA enrichment of *IAA19* and *YUC8* by LEC1-MYC was attenuated in *pif4* mutants (Figure 5H).

In addition, gibberellic acid (GA) and brassinosteroids (BRs) promote hypocotyl elongation depending on PIFs activity, while PIF4 functions on hypocotyl growth at high temperature through mediating auxin biosynthesis (de Lucas et al., 2008; Feng et al., 2008; Franklin et al., 2011; Oh et al., 2012; Bernardo-García et al., 2014). Our observations demonstrated that, resembling that in *pif4*, the effect of GA or brassinolide on hypocotyl elongation was attenuated, and, by contrast, the synthetic auxin picloram largely rescued the short hypocotyl phenotype at high temperature in the *lec1-4* mutant (Supplemental Figures 11A to 11C). Collectively, these results strongly suggest that LEC1 and PIF4 function interdependently in the regulation of hypocotyl growth.

DISCUSSION

LEC1 acts as a central regulator in embryogenesis, and it also plays a distinct role in postembryonic growth in Arabidopsis (Meinke et al., 1994; West et al., 1994; Parcy et al., 1997; Lotan et al., 1998; Harada, 2001; Junker and Bäumlein, 2012). However, the molecular mechanism by which LEC1 regulates such nonembryonic development so far remains elusive. Here, we demonstrated that LEC1 promotes etiolation growth via protein-protein interaction with PIF4, one of the key transcriptional activators in etiolation. Similar to *pif4*, the *lec1* mutant exhibits defects in hypocotyl elongation and apical hook formation in darkness, while inducible overexpression of *LEC1* promotes hypocotyl elongation of seedlings (Figures 2E; Supplemental Figures 4A and 4B; Huq and Quail, 2002; Junker et al., 2012). Protein interaction

Figure 2. (continued).

(F) Hypocotyl length statistics of the wild type and *pER10:LEC1-MYC* seedlings shown in **(E)**. Data represent mean ± SD of at least 30 seedlings. Asterisk indicates significant difference between *pER10:LEC1-MYC* with estradiol and mock treatment ($P < 0.05$, by Student's *t* test).

(G) Estradiol-induced *LEC1* overexpression promotes the expression of hypocotyl elongation-related genes. Three-day-old *pER10:LEC1-MYC* seedlings were treated with 10 μM estradiol or mock-treated and immediately transferred to darkness for the indicated time. Relative gene expression was calculated by comparing the values to that at 0 h. *TUB2* was amplified as an internal control.

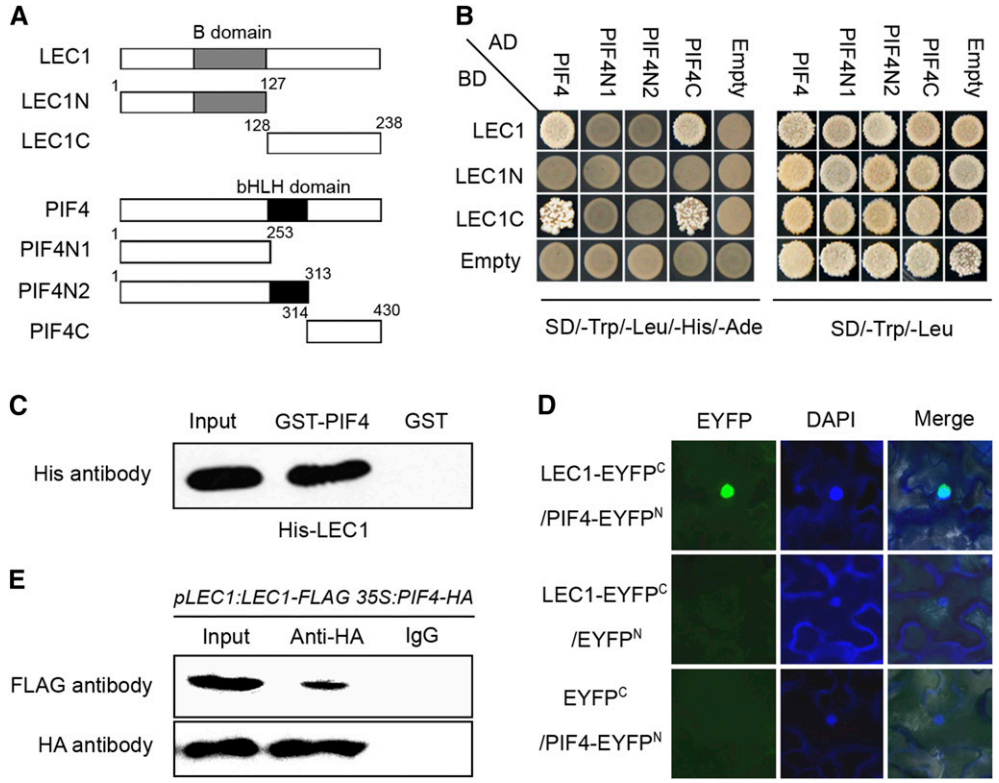

Figure 3. LEC1 Physically Interacts with PIF4 in Vitro and in Vivo.

(A) Sketches showing the domain structures of LEC1 and PIF4 and various deletions.

(B) Yeast two-hybrid assays showing the interactions between LEC1, PIF4, and their derivatives. Transformed yeast cells were grown on SD/-Trp/-Leu/-His/-Ade and SD/-Trp/-Leu medium.

(C) Pull-down assay showing direct interaction between His-LEC1 and GST-PIF4 fusion proteins in vitro. His-LEC1 protein was incubated with immobilized GST or GST-PIF4 proteins, and immunoprecipitated fractions were detected by anti-His antibody.

(D) BiFC assay showing LEC1-EYFP^C and PIF4-EYFP^N interact to form a functional EYFP in the nucleus. DAPI, fluorescence of 4′,6-diamidino-2-phenylindole; Merge, merge of EYFP and DAPI.

(E) In vivo interaction of PIF4 and LEC1 in Arabidopsis. Plant nuclear extracts from 5-d-old *pLEC1:LEC1-FLAG 35S:PIF4-HA* seedling grown in the dark were immunoprecipitated by either anti-HA antibody or preimmune serum (IgG). The coimmunoprecipitated proteins were detected by anti-FLAG antibody.

analyses, transient expression assays, EMSA, and ChIP analyses showed that LEC1 and PIF4 interdependently regulate hypocotyl elongation-related genes via direct binding to G-box in a dark-dependent manner. Corresponding to this, loss of *LEC1* function suppresses the elongated hypocotyl phenotype of *PIF*-over-accumulating plants, including *35S:PIF4*, *35S:PIF3-MYC*, and *phyb*; conversely, inducible overexpression of *LEC1* does not rescue the short hypocotyl phenotype of *pif4*. These results support a model in which LEC1 acts as a coactivator of PIFs in transcriptional regulation of postembryonic growth. Briefly, in the light, photoactivated phytochromes (Phy) interact with PIFs and trigger their code-gradation by the 26S proteasome, thus abolishing the expression of the etiolation-related genes and promoting photomorphogenesis. In the dark, LEC1 interacts with stabilized PIF4 to coregulate the etiolation-related genes via direct binding to the G-box, thus promoting skotomorphogenic growth (Figure 6). The transition from embryonic phase to seedling establishment is crucial for successful sporophyte development of plants. Because LEC1 plays indispensable roles in embryogenesis and postgerminative growth, both of which involve specification of hypocotyl and cotyledon development, this model provides new insights into the possible mechanism by which plants fine-tune morphological development for their survival during the seed-seedling switch when facing adverse conditions such as a lack of light.

LEC1 expression in dark-grown seedlings was previously reported (Warpeha et al., 2007; Siefers et al., 2009). In this study, however, we showed that *LEC1* expressed at comparable levels in seedlings grown in the light and the dark. Because *lec1* mutants also have shorter hypocotyls than the wild type in light-grown seedlings, in which no PIF4 protein was detected in contrast to its significant accumulation in the dark-grown seedlings (Figure 1F; Supplemental Figure 12), combined the observation that inducible LEC1 had no effect on the expression of downstream genes of PIF4 in the light (Supplemental Figures 3C and 3D), we cannot exclude the possibility that LEC1 plays an extra role in the light via a PIF4-independent mechanism.

GA mediates hypocotyl elongation through the interaction between DELLA proteins, the key GA signaling repressors, and

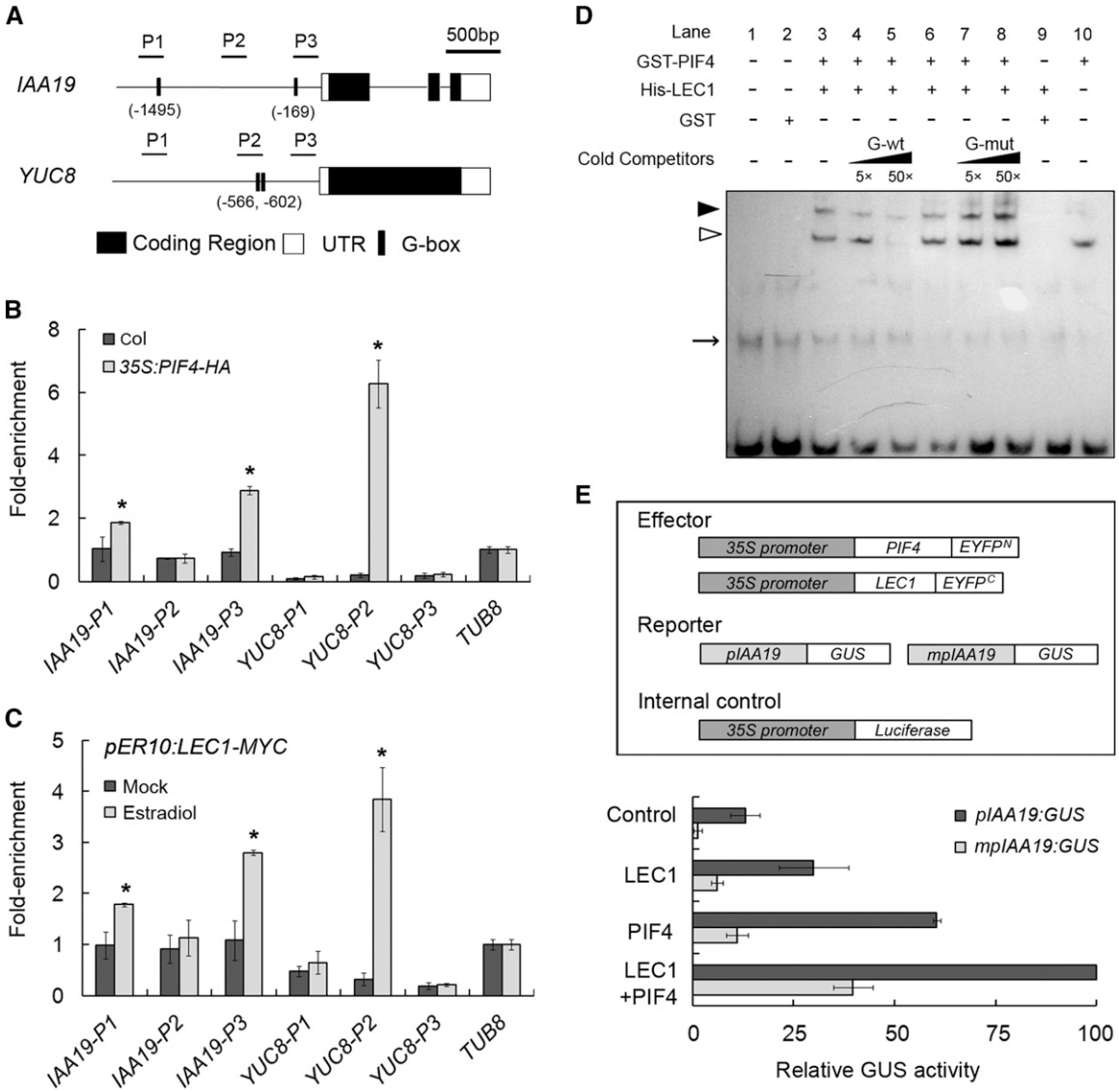

Figure 4. LEC1 and PIF4 Coregulate the Hypocotyl Elongation-Related Genes via Directly Binding to the G-Box.

(A) Schematic diagram of the *IAA19* and *YUC8* genomic regions. P1 to P3 indicate fragments for ChIP-qPCR amplification. Numbers indicate the positions of G-box elements in *IAA19* and *YUC8* promoters relative to ATG.

(B) ChIP analysis of PIF4-HA binding to G-box containing region in *IAA19* and *YUC8* genes upon precipitation with anti-HA antibody. Three-day-old of *35S:PIF4-HA* and Col seedlings were transferred to darkness for an additional 2 d and harvested for ChIP assay. Data represent mean ± SD of triplicates. Asterisks indicate significant changes in ChIP enrichment in *35S:PIF4-HA* compared with the Col sample ($P < 0.05$, by Student's *t* test).

(C) ChIP analysis of LEC1-MYC binding to the G-box containing region in *IAA19* and *YUC8* genes upon precipitation with anti-MYC antibody. Three-day-old of *pER10:LEC1-MYC* seedlings were treated with 10 μM estradiol or mock and immediately transferred to darkness for an additional two days and harvested for ChIP assay. Data represent mean ± SD of triplicates. Asterisks indicate significant changes in ChIP enrichment in estradiol-treated sample compared with the mock-treated sample ($P < 0.05$, by Student's *t* test).

(D) EMSA assay of the PIF4-LEC1 complex binding to the G-box in *IAA19* promoter (P3 region). The biotinylated probe containing the G-box element was incubated with GST-PIF4 (Lane 10), His-LEC1 (Lane 9), or their mixture (lanes 3 to 8), while the probe incubated with no protein (lane 1) or GST protein (lane 2) was used as negative control. Nonlabeled probes in 5- and 50-fold molar excess relative to the biotinylated probe containing G-box (G-wt, CACGTG) or mutated G-box (G-mut, CACGGG), respectively, were used as cold competitors. White and black arrowheads indicate the specific bindings of PIF4 protein and PIF4-LEC1 complex to the biotinylated probe, respectively, while arrow indicates nonspecific bands.

(E) Transient expression assays of *IAA19* transcriptional activity modulated by LEC1 and PIF4 in Arabidopsis mesophyll protoplasts. Various constructs used in transient expression assays are shown in the upper panel. Either *pIAA19:GUS* or *mpIAA19:GUS* was cotransformed with effectors or empty vector (Control) into Col mesophyll protoplasts. Relative GUS activity (GUS/Luciferase) that indicates the level of *IAA19* expression activated by various effectors is shown in the lower panel. Values are mean ± SD of five biological replicates.

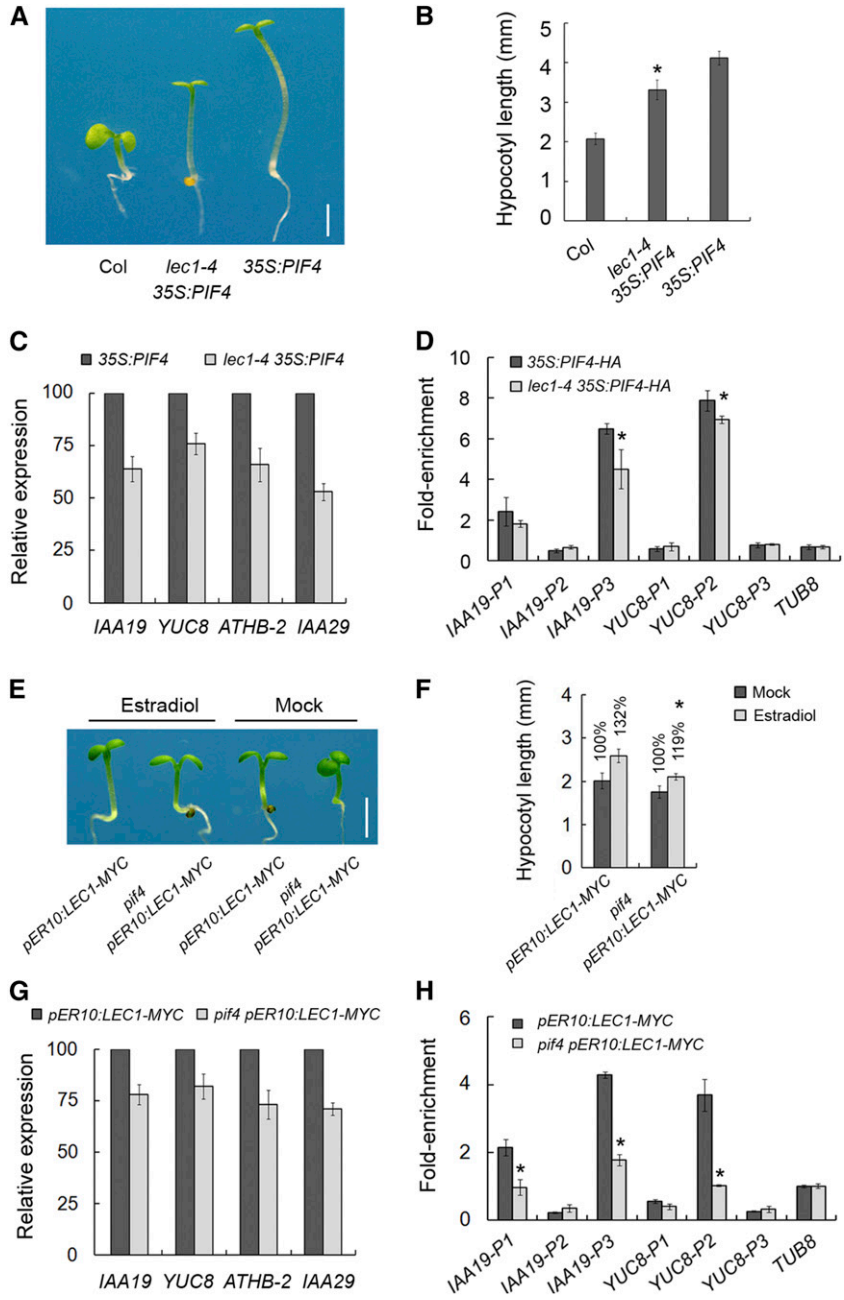

Figure 5. LEC1 Is Required for PIF4-Mediated Hypocotyl Elongation.

(A) Hypocotyl lengths of the wild-type, *35S:PIF4*, and *lec1-4 35S:PIF4* plants. Five-day-old seedlings grown in the light were used for investigation. Bar = 2 mm.

(B) Hypocotyl length statistics of the wild-type, *35S:PIF4*, and *lec1-4 35S:PIF4* seedlings shown in **(A)**. Data represent mean ± SD of at least 30 seedlings. Asterisks indicate significant difference between *35S:PIF4* and *lec1-4 35S:PIF4* ($P < 0.05$, by Student's *t* test).

(C) Quantitative RT-PCR analysis showing hypocotyl elongation-related genes expression in *35S:PIF4* and *lec1-4 35S:PIF4*. Three-day-old seedlings grown in the light were transferred to darkness for 6 h and then harvested for RNA extraction and further analysis. Relative gene expression levels were normalized against the expression of *TUB2* and those in *35S:PIF4* seedlings were designated as 100%.

(D) ChIP analysis of PIF4-HA binding to G-box containing region in *IAA19* and *YUC8* genes upon precipitation with anti-HA antibody. Three-day-old *35S:PIF4-HA* and *lec1-4 35S:PIF4-HA* seedlings were transferred to darkness for an additional 2 d and harvested for ChIP assay. Data represent mean ± SD of triplicates. Asterisks indicate significant changes in ChIP enrichment in *lec1-4 35S:PIF4-HA* compared with *35S:PIF4-HA* sample ($P < 0.05$, by Student's *t* test).

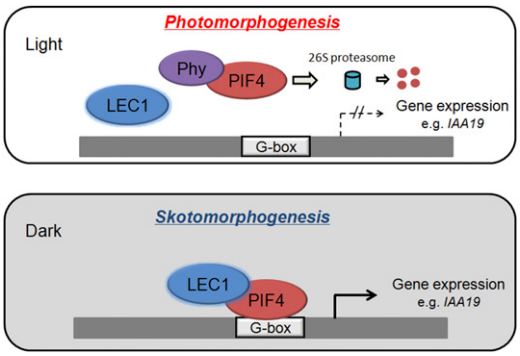

Figure 6. A Model Illustrating the Proposed Role of LEC1 and PIF4 in the Transcriptional Regulation during Postembryonic Growth.

In the light, photoactivated phytochromes (Phy) interact with PIF4 and trigger their codegradation by the 26S proteasome, thus abolishing the expression of the etiolation-related genes and promoting photomorphogenesis. In the dark, LEC1 interacts with stabilized PIF4 to coregulate the etiolation-related genes via direct binding to the G-box, thus promoting skotomorphogenic growth.

PIFs (de Lucas et al., 2008; Feng et al., 2008), while BR promotes hypocotyl elongation through PIF activity (Oh et al., 2012; Bernardo-García et al., 2014). Moreover, PIF4 promotes hypocotyl elongation at high temperature by mediating auxin biosynthesis (Franklin et al., 2011). Notably, a recent study showed that ectopically expressed LEC1 from an inducible *35S:LEC1-GR* transgene regulates the expression of the auxin synthesis gene *YUC10* and IAA accumulation in the elongation zone at hypocotyl-root junction, as well as the expression of genes involved in BR metabolism (Junker et al., 2012). We demonstrate that like PIF4, LEC1 also mediates GA and BR effects on the promotion of hypocotyl growth, while the synthetic auxin picloram significantly rescues the short hypocotyl phenotype responding to high temperature in both *pif4* and *lec1* (Supplemental Figure 11). Combined with the fact that LEC1 and PIF4 cotarget auxin-responsive genes, such as *IAA19* and *YUC8*, these findings further confirm the interdependent regulation of LEC1 and PIF4 presented in this model.

Seed embryos of *LEC1* null mutants are desiccation-intolerant and have to be rescued prior to desiccation for producing seedlings, causing problems in maintenance of homozygous recessive plants (West et al., 1994). In this study, we identified a *lec1* mutant, designated *lec1-4*, in which *LEC1* transcripts remain at a low level compared with that in the wild type. The *lec1-4* mutants show typical pleiotropic phenotypes in *LEC1* null alleles, including defective embryo, abnormal seeds, and postgerminative growth. More importantly, most *lec1-4* embryos are tolerant to desiccation so that ~90% of freshly harvested mutant seeds are viable, in spite that longer storage gradually reduces the germination rate. Because of the convenience in producing *lec1* homozygous plants, this allele provides an efficient genetic tool for us to learn how *LEC1* functions in plant development.

LEC1 encodes a protein related to the B-domain of NF-Y subunit, which can interact with NF-YC subunits and subsequently with the NF-YA subunit to form a heterotrimer binding to the CCAAT box (Calvenzani et al., 2012; Hackenberg et al., 2012). A de novo motif search showed that two motifs, the G-box-containing motif and the CCAAT box motif, are overrepresented in putative LEC1 target genes (Junker et al., 2012). However, disruption of the G-box but not the CCAAT box abolished the activation of seed storage-related genes by NF-YC2/bZIP67/LEC1 (or L1L) in mesophyll protoplasts (Yamamoto et al., 2009; Mendes et al., 2013). In this study, we demonstrate that the association with the G-box via PIFs is necessary for LEC1 to promote the expression of genes in response to skotomorphogenic growth. Although we observed no obvious binding of LEC1 to CCAAT in hypocotyl elongation-related genes in ChIP assays, whether the potentially functional CCAAT box is involved in LEC1-PIF regulation still needs further investigation.

To survive in the dark, seedlings undergo skotomorphogenesis by a complicated regulatory mechanism. Our findings shed light on the mechanism of LEC1-PIF module function in dark-adapted responses. However, studies have shown that PIFs also interact with several central regulators in multiple signals, which allows the integration of light and other cellular pathways to fine-tune plant growth (de Lucas et al., 2008; Feng et al., 2008; Oh et al., 2012; Liu et al., 2013; Zhang et al., 2014). The relationship between LEC1 and these regulators in early development of seedlings needs to be clarified. In addition, since LEC1 acts a key regulator in embryo development, including embryonic hypocotyl elongation, which was impaired in the *lec1* mutant (West et al., 1994), and some bHLH transcriptional factors function in embryo development (Kondou et al., 2008; Chandler et al., 2009; Sun et al., 2010), these findings indicate that a LEC1-PIF-like regulatory interaction could occur between LEC1 and other bHLHs in embryogenesis. Further

Figure 5. (continued).

(E) Hypocotyl lengths of *pER10:LEC1-MYC* and *pif4 pER10:LEC1-MYC* transgenic line. Five-day-old seedlings grown in the light with 10 μM estradiol or mock treatment were used for investigation. Bar = 2 mm.
(F) Hypocotyl length statistics of *pER10:LEC1-MYC* and *pif4 pER10:LEC1-MYC* shown in **(E)**. The percentage indicates the relative hypocotyl length with estradiol treatment against that with mock treatment (designated as 100%). Data represent mean ± SD of at least 30 seedlings. Asterisks indicate significant difference of relative hypocotyl length in *pif4 pER10:LEC1-MYC* compared with *pER10:LEC1-MYC* seedlings ($P < 0.05$, by Student's *t* test).
(G) Quantitative RT-PCR analysis showing expression of hypocotyl elongation-related genes in *pER10:LEC1-MYC* and *pif4 pER10:LEC1-MYC*. Three-day-old seedlings were treated with 10 μM estradiol and immediately transferred to darkness for 3 h and then harvested for RNA extraction and further analysis. Relative gene expression levels were normalized against the expression of *TUB2* and those in *pER10:LEC1-MYC* seedlings were designated as 100%.
(H) ChIP analysis of LEC1-MYC binding to G-box-containing region in *IAA19* and *YUC8* genes upon precipitation with anti-HA antibody. Three-day-old *pER10:LEC1-MYC* and *pif4 pER10:LEC1-MYC* seedlings were treated with 10 μM estradiol and immediately transferred to darkness for additional 2 d and harvested for ChIP experiment. Data represent mean ± SD of triplicates. Asterisks indicate significant changes in ChIP enrichment in *pif4 pER10:LEC1-MYC* compared with *pER10:LEC1-MYC* sample ($P < 0.05$, by Student's *t* test).

investigation of these issues will provide a comprehensive understanding of LEC1 functions in plant development.

METHODS

Plant Materials and Growth Conditions

The used plant materials including *lec1-3* (Sugliani et al., 2009), *pif4-2* (Sun et al., 2012), *pifq* (Zhang et al., 2013), *phyb-9* (Reed et al., 1993), *35S:PIF4-HA* (de Lucas et al., 2008), *35S:PIF4* (de Lucas et al., 2008), and *35S:PIF3-MYC* (Zhang et al., 2013) were previously described. All *Arabidopsis thaliana* plants used in this study are in Col background except *lec1-3*, which is in the Landsberg *erecta* background. The *lec1-4* (SALK_095699) and *l1l-1* (SALK_118236) mutant seeds were obtained from the ABRC. For experiment analyses, sterilized seeds sown on half-strength Murashige and Skoog (MS) medium containing no sucrose were incubated at 4°C in darkness for 3 d and then transferred to 22°C under full-spectrum white fluorescent light (16 h light/8 h dark) or in the dark for treatments as indicated.

Plasmid Construction and Plant Transformation

For the *pLEC1:LEC1-FLAG* construct, the 3.8-kb genomic fragment of *LEC1* without stop codon and 3′ untranslated region was amplified and cloned into the pPZPY122-FLAG binary vector (Hou et al., 2010). For *pLEC1:GUS* construct, ~2 kb promoter of *LEC1* was cloned into pCAMBIA 1391Z vector. The estradiol-inducible *pER10:LEC1-MYC* construct was previously described (Mu et al., 2008). Primers used for plasmid construction are listed in Supplemental Table 1. Transgenic plants harboring *pLEC1:LEC1-FLAG*, *pLEC1:GUS*, or *pER10:LEC1-MYC* were selected on half-strength MS medium supplemented with gentamycin, hygromycin, or kanamycin, respectively.

Hypocotyl Length Analysis

Seedlings grown on half-strength MS medium were photographed with a digital camera. The hypocotyl length was measured by Digimizer Image Analysis software.

Gene Expression Analysis

Growth conditions and treatment of seedlings were described in the text. Total RNA was extracted using the Plant RNA Kit (OMEGA) and reverse transcribed using the M-MLV reverse transcriptase (Promega). Quantitative PCR was performed in triplicates with the SYBR Premix ExTaq Mix (Takara Bio) following the manufacturer's instructions. The relative expression level was normalized to that of a *TUB2* internal control. Primers used for gene expression analysis are listed in Supplemental Table 1.

Yeast Two-Hybrid Assay

The coding regions of *LEC1*, *L1L*, and *PIFs* or truncated versions of *LEC1* and *PIF4* were amplified and cloned into pGBKT7 and pGADT7 (Clontech), respectively. Primers used are listed in Supplemental Table 1. Yeast two-hybrid assays were performed using the Yeastmaker Yeast Transformation System 2 (Clontech). Yeast AH109 cells were cotransformed with specific bait and prey constructs. All yeast transformants were grown on SD/-Trp/-Leu/-His/-Ade medium for selection or interaction tests.

Pull-Down and Coimmunoprecipitation

Full-length cDNAs of *PIF4* and *LEC1* were cloned into pGEX-4T-1 (Pharmacia) and pQE30 (Qiagen) vectors to produce GST-PIF4 and His-LEC1 proteins, respectively. Primers used for the construction are listed in Supplemental Table 1. GST and His fusion recombinant proteins were induced by isopropyl β-D-1-thiogalactopyranoside and expressed in *Escherichia coli* Rosetta (DE3; Novagen). The soluble GST and His fusion proteins were purified using Glutathione Sepharose Beads (Amersham Biosciences) or Ni-NTA agarose beads (Qiagen), following the manufacturers' instructions. For pull-down assays, 2 μg His-LEC1 was incubated in the binding buffer (50 mM Tris-HCl, pH 8.0, 100 mM NaCl, and 1 mM EDTA) with immobilized GST or GST fusion protein at 4°C for 2 h. After washing with binding buffer, proteins retained on the beads were subsequently resolved by SDS-PAGE and detected with anti-His antibody (BGI). For coimmunoprecipitation, 3-d-old *pLEC1:LEC1-FLAG 35S:PIF4-HA* seedlings were kept in darkness for additional 2 d and then total proteins were extracted. Total proteins were extracted with extraction buffer (50 mM HEPES, pH 7.5, 150 mM NaCl, 5 mM DTT, and 1% Triton X-100). After centrifugation, the supernatants were incubated with anti-HA agarose conjugate (Sigma-Aldrich) in the coimmunoprecipitation buffer (50 mM HEPES, pH 7.5, 150 mM KCl, 10 μM $ZnSO_4$, 5 mM $MgCl_2$, and 1% Triton X-100) at 4°C for 2 h. After washing with coimmunoprecipitation buffer three times, the proteins bound to beads were resolved by SDS-PAGE and detected by anti-FLAG or anti-HA antibody (Santa Cruz Biotechnology).

BiFC Assay

Full-length cDNAs of *LEC1* and *PIF4* were cloned into the pGreen binary vector HY105 containing C- or N-terminal fusions of EYFP to generate *35S:LEC1-EYFP^C* and *35S:PIF4-EYFP^N*, then cotransformed into tobacco (*Nicotiana benthamiana*) leaf epidermal cells by infiltration as previously published (Hou et al., 2014). After infiltration, tobacco was grown for 2 d and transferred to darkness for 24 h before detection of the YFP signals. The YFP fluorescence was determined using a fluorescence microscope (Leica). DAPI (4',6-diamidino-2-phenylindole) staining was used to show the nucleus.

ChIP Assay

ChIP assays were performed as previously described (Hou et al., 2014). Briefly, for *35S:PIF4-HA*, 3-d-old seedlings were transferred to darkness for additional 2 d and harvested for fixation. For *pER10:LEC1-MYC*, 3-d-old seedlings were treated with 10 μM estradiol and immediately transferred to darkness for additional 2 d and harvested for fixation. Chromatin was isolated and sonicated to generate DNA fragment with an average size of ~500 bp. The solubilized chromatin was immunoprecipitated by Protein G PLUS agarose (Santa Cruz Biotechnology) with anti-HA (Santa Cruz Biotechnology), anti-MYC (Santa Cruz Biotechnology), and the coimmunoprecipitated DNA was recovered and analyzed by quantitative PCR with SYBR Premix ExTaq Mix (Takara Bio). Relative fold-enrichment was calculated by normalizing the amount of a target DNA fragment against that of a *TUB8* genomic fragment and then against the respective input DNA samples. The primers used are listed in Supplemental Table 1.

EMSA

The EMSA assay was performed using the LightShift Chemiluminescent EMSA kit (Pierce). The 5′-end biotinylated oligonucleotide containing G-box in the P3 region of *IAA19* promoter was used as a probe, while nonlabeled probe containing the native G-box (CACGTG) or mutated G-box (CACGgG) was used as cold competitor (Supplemental Figure 8A). Recombinant His-LEC1 and GST-PIF4 proteins were used for protein-DNA binding.

Transient Expression Assay

To generate the *pIAA19:GUS* reporter construct, ~2 kb *IAA19* promoter was cloned into HY107-containing GUS gene (Hou et al., 2014). *mpIAA19:GUS* carrying two mutated G-box elements (CACGTG to CACGGG) was generated by overlapping PCR reaction from *pIAA19:GUS* construct (Supplemental Figure 8B). *35S:LEC1-EYFP^C* and *35S:PIF4-EYFP^N* were used as effector constructs and a construct containing the firefly luciferase

driven by 35S promoter in pGreen-35S was used as an internal control to evaluate the protoplast transfection efficiency. All primers used for generating constructs for transient expression assays are listed in Supplemental Table 1. Arabidopsis mesophyll protoplasts were prepared, transfected, and cultured as previously described (Yoo et al., 2007). Relative GUS activity was calculated by normalizing against the luciferase activity, and the data presented are the averages of five biological replicates.

Accession Numbers

Sequence data from this article can be found in the Arabidopsis Genome Initiative database under the following accession numbers: *LEC1* (AT1G21970), *L1L* (AT5G47670), *PIF3* (AT1g09530), *PIF4* (AT2G43010), *IAA19* (AT3G15540), *ATHB-2* (AT4G16780), *YUC8* (AT4G28720), *IAA29* (AT4G32280), *TUB2* (AT5G62690), and *TUB8* (At5g23860).

Supplemental Data

Supplemental Figure 1. Characterization of the *lec1-4* Mutant.

Supplemental Figure 2. *pLEC1:LEC1-FLAG* Complements Growth Defects of *lec1-4*.

Supplemental Figure 3. Characterization of *pER10:LEC1-MYC* Transgenic Line.

Supplemental Figure 4. Hypocotyl Length and Gene Expression Analysis in *lec1-4*, *pif4*, *pifq*, and *pER10:LEC1-MYC* Transgenic Plants.

Supplemental Figure 5. Yeast Two-Hybrid Assays Showing the Interactions between LEC1, L1L, and PIFs.

Supplemental Figure 6. Hypocotyl Phenotype of the *l1l-1* Mutant.

Supplemental Figure 7. ChIP Analysis of LEC1-MYC Binding in *IAA29* and *ATHB-2* Genes in the Dark and Light.

Supplemental Figure 8. Mutated Versions of the *IAA19* Sequence Used in EMSA and Transient Expression Assays.

Supplemental Figure 9. Transient Expression Assays of *IAA19* Transcriptional Activity Modulated by LEC1.

Supplemental Figure 10. *lec1-4* Suppresses the Long Hypocotyl Phenotype of *35S:PIF3-MYC* and *phyb*.

Supplemental Figure 11. Effects of GA, Auxin, and BR on Hypocotyl Elongation of *lec1-4* and *pif4*.

Supplemental Figure 12. Immunoblot Analysis of PIF4 Protein.

Supplemental Table 1. List of Primers Used in This Study.

ACKNOWLEDGMENTS

We thank C. Fankhauser for providing *35S:PIF4-HA* seeds, C. Li for *pif4-2* seeds, W.J.J. Soppe for *lec1-3* seeds, J. Li for *bri1-301* seeds, the ABRC for *lec1-4* and *l1l-1* seeds, J. Zuo for *pER10:LEC1-MYC* plasmid, and W. Xi and H. Yu for critical reading of the manuscript. This work was supported by grants from the National Natural Science Foundation of China (31370342, 31301055, and 31300239), the "Hundred Talents" program of the Chinese Academy of Sciences, and the Natural Science Foundation of Guangdong Province (S2013010014954 and S2013040013147).

AUTHOR CONTRIBUTIONS

M.H. and X.H. designed the research. M.H., Y.H., X.L., and Y.L. performed research. M.H., Y.H., and X.H. analyzed data. M.H. and X.H. wrote the article.

Received August 25, 2015; revised October 14, 2015; accepted October 22, 2015; published November 13, 2015.

REFERENCES

Al-Sady, B., Ni, W., Kircher, S., Schäfer, E., and Quail, P.H. (2006). Photoactivated phytochrome induces rapid PIF3 phosphorylation prior to proteasome-mediated degradation. Mol. Cell **23:** 439–446.

Bae, G., and Choi, G. (2008). Decoding of light signals by plant phytochromes and their interacting proteins. Annu. Rev. Plant Biol. **59:** 281–311.

Bernardo-García, S., de Lucas, M., Martínez, C., Espinosa-Ruiz, A., Davière, J.M., and Prat, S. (2014). BR-dependent phosphorylation modulates PIF4 transcriptional activity and shapes diurnal hypocotyl growth. Genes Dev. **28:** 1681–1694.

Brocard-Gifford, I.M., Lynch, T.J., and Finkelstein, R.R. (2003). Regulatory networks in seeds integrating developmental, abscisic acid, sugar, and light signaling. Plant Physiol. **131:** 78–92.

Calvenzani, V., Testoni, B., Gusmaroli, G., Lorenzo, M., Gnesutta, N., Petroni, K., Mantovani, R., and Tonelli, C. (2012). Interactions and CCAAT-binding of *Arabidopsis thaliana* NF-Y subunits. PLoS One **7:** e42902.

Castillon, A., Shen, H., and Huq, E. (2007). Phytochrome Interacting Factors: central players in phytochrome-mediated light signaling networks. Trends Plant Sci. **12:** 514–521.

Chandler, J.W., Cole, M., Flier, A., and Werr, W. (2009). BIM1, a bHLH protein involved in brassinosteroid signalling, controls *Arabidopsis* embryonic patterning via interaction with DORNROSCHEN and DORNROSCHEN-LIKE. Plant Mol. Biol. **69:** 57–68.

Chen, M., Chory, J., and Fankhauser, C. (2004). Light signal transduction in higher plants. Annu. Rev. Genet. **38:** 87–117.

de Lucas, M., Davière, J.M., Rodríguez-Falcón, M., Pontin, M., Iglesias-Pedraz, J.M., Lorrain, S., Fankhauser, C., Blázquez, M.A., Titarenko, E., and Prat, S. (2008). A molecular framework for light and gibberellin control of cell elongation. Nature **451:** 480–484.

Feng, S., et al. (2008). Coordinated regulation of *Arabidopsis thaliana* development by light and gibberellins. Nature **451:** 475–479.

Franklin, K.A., Lee, S.H., Patel, D., Kumar, S.V., Spartz, A.K., Gu, C., Ye, S., Yu, P., Breen, G., Cohen, J.D., Wigge, P.A., and Gray, W.M. (2011). Phytochrome-interacting factor 4 (PIF4) regulates auxin biosynthesis at high temperature. Proc. Natl. Acad. Sci. USA **108:** 20231–20235.

Hackenberg, D., Wu, Y., Voigt, A., Adams, R., Schramm, P., and Grimm, B. (2012). Studies on differential nuclear translocation mechanism and assembly of the three subunits of the *Arabidopsis thaliana* transcription factor NF-Y. Mol. Plant **5:** 876–888.

Harada, J.J. (2001). Role of *Arabidopsis* LEAFY COTYLEDON genes in seed development. J. Plant Physiol. **158:** 405–409.

Hornitschek, P., Kohnen, M.V., Lorrain, S., Rougemont, J., Ljung, K., López-Vidriero, I., Franco-Zorrilla, J.M., Solano, R., Trevisan, M., Pradervand, S., Xenarios, I., and Fankhauser, C. (2012). Phytochrome interacting factors 4 and 5 control seedling growth in changing light conditions by directly controlling auxin signaling. Plant J. **71:** 699–711.

Hou, X., Lee, L.Y.C., Xia, K., Yan, Y., and Yu, H. (2010). DELLAs modulate jasmonate signaling via competitive binding to JAZs. Dev. Cell **19:** 884–894.

Hou, X., Zhou, J., Liu, C., Liu, L., Shen, L., and Yu, H. (2014). Nuclear factor Y-mediated H3K27me3 demethylation of the SOC1 locus orchestrates flowering responses of *Arabidopsis.* Nat. Commun. **5:** 4601.

Huq, E., and Quail, P.H. (2002). PIF4, a phytochrome-interacting bHLH factor, functions as a negative regulator of phytochrome B signaling in *Arabidopsis.* EMBO J. **21:** 2441–2450.

Jing, Y., Zhang, D., Wang, X., Tang, W., Wang, W., Huai, J., Xu, G., Chen, D., Li, Y., and Lin, R. (2013). *Arabidopsis* chromatin remodeling factor PICKLE interacts with transcription factor HY5 to regulate hypocotyl cell elongation. Plant Cell **25:** 242–256.

Josse, E.M., and Halliday, K.J. (2008). Skotomorphogenesis: the dark side of light signalling. Curr. Biol. **18:** R1144–R1146.

Junker, A., and Bäumlein, H. (2012). Multifunctionality of the LEC1 transcription factor during plant development. Plant Signal. Behav. **7:** 1718–1720.

Junker, A., et al. (2012). Elongation-related functions of LEAFY COTYLEDON1 during the development of *Arabidopsis thaliana*. Plant J. **71:** 427–442.

Khanna, R., Huq, E., Kikis, E.A., Al-Sady, B., Lanzatella, C., and Quail, P.H. (2004). A novel molecular recognition motif necessary for targeting photoactivated phytochrome signaling to specific basic helix-loop-helix transcription factors. Plant Cell **16:** 3033–3044.

Kim, J., Yi, H., Choi, G., Shin, B., Song, P.S., and Choi, G. (2003). Functional characterization of phytochrome interacting factor 3 in phytochrome-mediated light signal transduction. Plant Cell **15:** 2399–2407.

Kondou, Y., Nakazawa, M., Kawashima, M., Ichikawa, T., Yoshizumi, T., Suzuki, K., Ishikawa, A., Koshi, T., Matsui, R., Muto, S., and Matsui, M. (2008). RETARDED GROWTH OF EMBRYO1, a new basic helix-loop-helix protein, expresses in endosperm to control embryo growth. Plant Physiol. **147:** 1924–1935.

Kunihiro, A., Yamashino, T., Nakamichi, N., Niwa, Y., Nakanishi, H., and Mizuno, T. (2011). Phytochrome-interacting factor 4 and 5 (PIF4 and PIF5) activate the homeobox ATHB2 and auxin-inducible IAA29 genes in the coincidence mechanism underlying photoperiodic control of plant growth of *Arabidopsis thaliana*. Plant Cell Physiol. **52:** 1315–1329.

Le, B.H., et al. (2010). Global analysis of gene activity during *Arabidopsis* seed development and identification of seed-specific transcription factors. Proc. Natl. Acad. Sci. USA **107:** 8063–8070.

Leivar, P., and Monte, E. (2014). PIFs: systems integrators in plant development. Plant Cell **26:** 56–78.

Leivar, P., and Quail, P.H. (2011). PIFs: pivotal components in a cellular signaling hub. Trends Plant Sci. **16:** 19–28.

Leivar, P., Monte, E., Oka, Y., Liu, T., Carle, C., Castillon, A., Huq, E., and Quail, P.H. (2008). Multiple phytochrome-interacting bHLH transcription factors repress premature seedling photomorphogenesis in darkness. Curr. Biol. **18:** 1815–1823.

Liu, J.X., and Howell, S.H. (2010). bZIP28 and NF-Y transcription factors are activated by ER stress and assemble into a transcriptional complex to regulate stress response genes in *Arabidopsis*. Plant Cell **22:** 782–796.

Liu, X., Chen, C.Y., Wang, K.C., Luo, M., Tai, R., Yuan, L., Zhao, M., Yang, S., Tian, G., Cui, Y., Hsieh, H.L., and Wu, K. (2013). PHYTOCHROME INTERACTING FACTOR3 associates with the histone deacetylase HDA15 in repression of chlorophyll biosynthesis and photosynthesis in etiolated *Arabidopsis* seedlings. Plant Cell **25:** 1258–1273.

Lotan, T., Ohto, M., Yee, K.M., West, M.A., Lo, R., Kwong, R.W., Yamagishi, K., Fischer, R.L., Goldberg, R.B., and Harada, J.J. (1998). *Arabidopsis* LEAFY COTYLEDON1 is sufficient to induce embryo development in vegetative cells. Cell **93:** 1195–1205.

Meinke, D.W., Franzmann, L.H., Nickle, T.C., and Yeung, E.C. (1994). Leafy cotyledon mutants of *Arabidopsis*. Plant Cell **6:** 1049–1064.

Mendes, A., Kelly, A.A., van Erp, H., Shaw, E., Powers, S.J., Kurup, S., and Eastmond, P.J. (2013). bZIP67 regulates the omega-3 fatty acid content of *Arabidopsis* seed oil by activating fatty acid desaturase3. Plant Cell **25:** 3104–3116.

Mu, J., Tan, H., Zheng, Q., Fu, F., Liang, Y., Zhang, J., Yang, X., Wang, T., Chong, K., Wang, X.J., and Zuo, J. (2008). LEAFY COTYLEDON1 is a key regulator of fatty acid biosynthesis in *Arabidopsis*. Plant Physiol. **148:** 1042–1054.

Ni, W., Xu, S.L., Tepperman, J.M., Stanley, D.J., Maltby, D.A., Gross, J.D., Burlingame, A.L., Wang, Z.Y., and Quail, P.H. (2014). A mutually assured destruction mechanism attenuates light signaling in *Arabidopsis*. Science **344:** 1160–1164.

Oh, E., Zhu, J.Y., and Wang, Z.Y. (2012). Interaction between BZR1 and PIF4 integrates brassinosteroid and environmental responses. Nat. Cell Biol. **14:** 802–809.

Parcy, F., Valon, C., Kohara, A., Miséra, S., and Giraudat, J. (1997). The ABSCISIC ACID-INSENSITIVE3, FUSCA3, and LEAFY COTYLEDON1 loci act in concert to control multiple aspects of *Arabidopsis* seed development. Plant Cell **9:** 1265–1277.

Reed, J.W., Nagpal, P., Poole, D.S., Furuya, M., and Chory, J. (1993). Mutations in the gene for the red/far-red light receptor phytochrome B alter cell elongation and physiological responses throughout *Arabidopsis* development. Plant Cell **5:** 147–157.

Siefers, N., Dang, K.K., Kumimoto, R.W., Bynum IV, W.E., Tayrose, G., and Holt III, B.F. (2009). Tissue-specific expression patterns of *Arabidopsis* NF-Y transcription factors suggest potential for extensive combinatorial complexity. Plant Physiol. **149:** 625–641.

Sugliani, M., Rajjou, L., Clerkx, E.J.M., Koornneef, M., and Soppe, W.J.J. (2009). Natural modifiers of seed longevity in the *Arabidopsis* mutants abscisic acid insensitive3-5 (abi3-5) and leafy cotyledon1-3 (lec1-3). New Phytol. **184:** 898–908.

Sun, J., Qi, L., Li, Y., Chu, J., and Li, C. (2012). PIF4-mediated activation of YUCCA8 expression integrates temperature into the auxin pathway in regulating *Arabidopsis* hypocotyl growth. PLoS Genet. **8:** e1002594.

Sun, X., Shantharaj, D., Kang, X., and Ni, M. (2010). Transcriptional and hormonal signaling control of *Arabidopsis* seed development. Curr. Opin. Plant Biol. **13:** 611–620.

Toledo-Ortiz, G., Huq, E., and Quail, P.H. (2003). The *Arabidopsis* basic/helix-loop-helix transcription factor family. Plant Cell **15:** 1749–1770.

Von Arnim, A., and Deng, X.W. (1996). Light control of seedling development. Annu. Rev. Plant Physiol. Plant Mol. Biol. **47:** 215–243.

Warpeha, K.M., Upadhyay, S., Yeh, J., Adamiak, J., Hawkins, S.I., Lapik, Y.R., Anderson, M.B., and Kaufman, L.S. (2007). The GCR1, GPA1, PRN1, NF-Y signal chain mediates both blue light and abscisic acid responses in *Arabidopsis*. Plant Physiol. **143:** 1590–1600.

West, M., Yee, K.M., Danao, J., Zimmerman, J.L., Fischer, R.L., Goldberg, R.B., and Harada, J.J. (1994). LEAFY COTYLEDON1 is an essential regulator of late embryogenesis and cotyledon identity in *Arabidopsis*. Plant Cell **6:** 1731–1745.

Yamamoto, A., Kagaya, Y., Toyoshima, R., Kagaya, M., Takeda, S., and Hattori, T. (2009). *Arabidopsis* NF-YB subunits LEC1 and LEC1-LIKE activate transcription by interacting with seed-specific ABRE-binding factors. Plant J. **58:** 843–856.

Yoo, S.D., Cho, Y.H., and Sheen, J. (2007). *Arabidopsis* mesophyll protoplasts: a versatile cell system for transient gene expression analysis. Nat. Protoc. **2:** 1565–1572.

Zhang, D., Jing, Y., Jiang, Z., and Lin, R. (2014). The chromatin-remodeling factor PICKLE integrates brassinosteroid and gibberellin signaling during skotomorphogenic growth in *Arabidopsis*. Plant Cell **26:** 2472–2485.

Zhang, H., Bishop, B., Ringenberg, W., Muir, W.M., and Ogas, J. (2012). The CHD3 remodeler PICKLE associates with genes enriched for trimethylation of histone H3 lysine 27. Plant Physiol. **159:** 418–432.

Zhang, Y., Mayba, O., Pfeiffer, A., Shi, H., Tepperman, J.M., Speed, T.P., and Quail, P.H. (2013). A quartet of PIF bHLH factors provides a transcriptionally centered signaling hub that regulates seedling morphogenesis through differential expression-patterning of shared target genes in *Arabidopsis*. PLoS Genet. **9:** e1003244.